A role for the PIWI domain in mediating interactions with the 5′ end of the guide RNA complements the function of the PAZ domain in recognizing RNA 3′ overhangs[7–10]. In *Pyrococcus furiosus* Argonaute, the PAZ domain is positioned over the channel linking the G1-binding pocket and the putative slicer site[11]. The PAZ domain may function as a mobile unit that locks down over the guide–target duplex, providing additional constraints for slicing[11]. However, when bound to a target mRNA, it is unlikely that the recessed guide 3′ end would interact with the PAZ domain[10]; instead, we envisage the duplex emerging into solvent or the immediate environment of RISC.

Our structure rationalizes many molecular and biochemical data for mechanisms of RNA silencing, which, together with the universal conservation of the G1-binding pocket, indicate that the AfPiwi–RNA complex provides a representative picture of PIWI domain–RNA interactions. The view now emerges that Argonaute functions as a dynamic molecule mediating interactions with both the 5′ and 3′ ends of short guide RNA molecules, presenting them for recognition by cognate mRNA.

Note added in proof: In an accompanying paper[31], Ma *et al.* use a different siRNA oligonucleotide to define the structure of an AfPiwi–RNA complex. Their structure is similar to ours, although less of the RNA molecule is defined. Consistent with our model for 5′-end guide recognition in eukaryotic Argonaute proteins, mutation of the G1-binding pocket in hAgo2 ablates slicer activity. □

Methods

Complex formation and crystallization

AfPiwi was purified as described[12], except that the protein was eluted at the final step in 5 mM HEPES pH 7.5, 800 mM NaCl, 2 mM $MgCl_2$, 1 mM $MnCl_2$, 8 mM dithiothreitol (DTT). The RNA oligonucleotide was purchased purified, deprotected and desalted from Dharmacon, and was resolubilized in 10 mM HEPES pH 7.5, 100 mM NaCl, 2 mM $MgCl_2$. Annealing was performed by incubation at 90 °C for 1 min followed by gradual cooling (1 °C per 5 min) from 65 °C to 4 °C. To form the complex, equal volumes of AfPiwi (260 μM) and annealed RNA (310 μM) were mixed and incubated at 22 °C for 30 min. Crystallization was performed with the hanging drop method at 14 °C. Crystal clusters were obtained overnight by mixing 1 μl of complex with 1 μl of 200 mM KCl, 10 mM $CaCl_2$, 50 mM sodium cacodylate pH 5.5, 15% PEG 4000, 5 mM DTT. Single crystals were obtained by streak-seeding into a similar drop containing 12% PEG 4000 after incubation overnight. For cryoprotection, crystals were passed through stabilization solutions containing increasing amounts of 2-methyl-2,4-pentane diol (to 17%) and then flash-frozen at 100 K. Data were collected at ID14.EH1, ESRF.

Structure determination

The structure (with two AfPiwi–RNA complexes per *P*1 unit cell) was solved by molecular replacement with PHASER[29] by using the native protein (PDB code 1W9H) as the search model[12]. Some loops and all the RNA were rebuilt manually in COOT[30] and the complex was refined with REFMAC[29]. A total of 508 water molecules were added in the final stages of refinement. The final R and R_{free} were 0.18 and 0.21, respectively (Supplementary Table 1). Terminal nucleotides of the target strands in the two RNA duplexes per unit cell adopt slightly different conformations (Supplementary Fig. 1). On the basis of crystallization conditions and refinement, we have assigned the metal ion within the G1-binding pocket as manganese.

Received 21 December 2004; accepted 17 February 2005; doi:10.1038/nature03462.

1. Mello, C. C. & Conte, D. Jr Revealing the world of RNA interference. *Nature* **431**, 338–342 (2004).
2. Meister, G. & Tuschl, T. Mechanisms of gene silencing by double-stranded RNA. *Nature* **431**, 343–349 (2004).
3. Carmell, M. A., Xuan, Z., Zhang, M. Q. & Hannon, G. J. The Argonaute family: tentacles that reach into RNAi, developmental control, stem cell maintenance, and tumorigenesis. *Genes Dev.* **16**, 2733–2742 (2002).
4. Hammond, S. M., Boettcher, S., Caudy, A. A., Kobayashi, R. & Hannon, G. J. Argonaute2, a link between genetic and biochemical analyses of RNAi. *Science* **293**, 1146–1150 (2001).
5. Verdel, A. *et al.* RNAi-mediated targeting of heterochromatin by the RITS complex. *Science* **303**, 672–676 (2004).
6. Sontheimer, E. J. Assembly and function of RNA silencing complexes. *Nature Rev. Mol. Cell Biol.* **6**, 127–138 (2005).
7. Yan, K. S. *et al.* Structure and conserved RNA binding of the PAZ domain. *Nature* **426**, 468–474 (2003).
8. Song, J. J. *et al.* The crystal structure of the Argonaute2 PAZ domain reveals an RNA binding motif in RNAi effector complexes. *Nature Struct. Biol.* **10**, 1026–1032 (2003).
9. Lingel, A., Simon, B., Izaurralde, E. & Sattler, M. Nucleic acid 3′-end recognition by the Argonaute2 PAZ domain. *Nature Struct. Mol. Biol.* **11**, 576–577 (2004).
10. Ma, J. B., Ye, K. & Patel, D. J. Structural basis for overhang-specific small interfering RNA recognition by the PAZ domain. *Nature* **429**, 318–322 (2004).
11. Song, J. J., Smith, S. K., Hannon, G. J. & Joshua-Tor, L. Crystal structure of Argonaute and its implications for RISC slicer activity. *Science* **305**, 1434–1437 (2004).
12. Parker, J. S., Roe, S. M. & Barford, D. Crystal structure of a PIWI protein suggests mechanisms for siRNA recognition and slicer activity. *EMBO J.* **23**, 4727–4737 (2004).
13. Liu, J. *et al.* Argonaute2 is the catalytic engine of mammalian RNAi. *Science* **305**, 1437–1441 (2004).
14. Nykanen, A., Haley, B. & Zamore, P. D. ATP requirements and small interfering RNA structure in the RNA interference pathway. *Cell* **107**, 309–321 (2001).
15. Chiu, Y. L. & Rana, T. M. RNAi in human cells: basic structural and functional features of small interfering RNA. *Mol. Cell* **10**, 549–561 (2002).
16. Martinez, J., Patkaniowska, A., Urlaub, H., Luhrmann, R. & Tuschl, T. Single-stranded antisense siRNAs guide target RNA cleavage in RNAi. *Cell* **110**, 563–574 (2002).
17. Elbashir, S. M., Martinez, J., Patkaniowska, A., Lendeckel, W. & Tuschl, T. Functional anatomy of siRNAs for mediating efficient RNAi in *Drosophila melanogaster* embryo lysate. *EMBO J.* **20**, 6877–6888 (2001).
18. Elbashir, S. M., Lendeckel, W. & Tuschl, T. RNA interference is mediated by 21- and 22-nucleotide RNAs. *Genes Dev.* **15**, 188–200 (2001).
19. Haley, B. & Zamore, P. D. Kinetic analysis of the RNAi enzyme complex. *Nature Struct. Mol. Biol.* **11**, 599–606 (2004).
20. Hutvagner, G. & Zamore, P. D. A microRNA in a multiple-turnover RNAi enzyme complex. *Science* **297**, 2056–2060 (2002).
21. Lewis, B. P., Shih, I. H., Jones-Rhoades, M. W., Bartel, D. P. & Burge, C. B. Prediction of mammalian microRNA targets. *Cell* **115**, 787–798 (2003).
22. Stark, A., Brennecke, J., Russell, R. B. & Cohen, S. M. Identification of *Drosophila* MicroRNA targets. *PLoS Biol.* **1**, 397–409 (2003).
23. Doench, J. G. & Sharp, P. A. Specificity of microRNA target selection in translational repression. *Genes Dev.* **18**, 504–511 (2004).
24. Lewis, B. P., Burge, C. B. & Bartel, D. P. Conserved seed pairing, often flanked by adenosines, indicates that thousands of human genes are MicroRNA targets. *Cell* **120**, 15–20 (2005).
25. Khvorova, A., Reynolds, A. & Jayasena, S. D. Functional siRNAs and miRNAs exhibit strand bias. *Cell* **115**, 209–216 (2003).
26. Schwarz, D. S. *et al.* Asymmetry in the assembly of the RNAi enzyme complex. *Cell* **115**, 199–208 (2003).
27. Okamura, K., Ishizuka, A., Siomi, H. & Siomi, M. C. Distinct roles for Argonaute proteins in small RNA-directed RNA cleavage pathways. *Genes Dev.* **18**, 1655–1666 (2004).
28. Tomari, Y., Matranga, C., Haley, B., Martinez, N. & Zamore, P. D. A protein sensor for siRNA asymmetry. *Science* **306**, 1377–1380 (2004).
29. Collaborative Computational Project No. 4. The CCP4 suite: programs for protein crystallography. *Acta Crystallogr. D* **50**, 760–763 (1994).
30. Emsley, P. & Cowtan, K. Coot: model-building tools for molecular graphics. *Acta Crystallogr. D* **60**, 2126–2132 (2004).
31. Ma, J.-B. *et al.* Structural basis for 5′-end-specific recognition of guide RNA by the *A. fulgidus* Piwi protein. *Nature* doi:10.1038/nature03514 (this issue).

Supplementary Information accompanies the paper on **www.nature.com/nature**.

Acknowledgements We are grateful to staff at ESRF for help with data collection. The work was funded by Cancer Research–UK, the Wellcome Trust and the Institute of Cancer Research.

Competing interests statement The authors declare that they have no competing financial interests.

Correspondence and requests for materials should be addressed to D.B. (david.barford@icr.ac.uk). The coordinates and structure factors have been deposited with the Protein Data Bank with accession numbers 2bgg and r2bggsf, respectively.

Structural basis for 5′-end-specific recognition of guide RNA by the *A. fulgidus* Piwi protein

Jin-Biao Ma[1], Yu-Ren Yuan[1], Gunter Meister[2], Yi Pei[2], Thomas Tuschl[2] & Dinshaw J. Patel[1]

[1]*Structural Biology Program, Memorial Sloan-Kettering Cancer Center, New York, New York 10021, USA*
[2]*Laboratory of RNA Molecular Biology, The Rockefeller University, New York, New York 10021, USA*

RNA interference (RNAi) is a conserved sequence-specific gene regulatory mechanism[1–3] mediated by the RNA-induced silencing complex (RISC), which is composed of a single-stranded guide RNA and an Argonaute protein. The PIWI domain, a highly conserved motif within Argonaute, has been shown to adopt an RNase H fold[4,5] critical for the endonuclease cleavage activity of

RISC[4–6]. Here we report the crystal structure of *Archaeoglobus fulgidus* Piwi protein bound to double-stranded RNA, thereby identifying the binding pocket for guide-strand 5′-end recognition and providing insight into guide-strand-mediated messenger RNA target recognition. The phosphorylated 5′ end of the guide RNA is anchored within a highly conserved basic pocket, supplemented by the carboxy-terminal carboxylate and a bound divalent cation. The first nucleotide from the 5′ end of the guide RNA is unpaired and stacks over a conserved tyrosine residue, whereas successive nucleotides form a four-base-pair RNA duplex. Mutation of the corresponding amino acids that contact the 5′ phosphate in human Ago2 resulted in attenuated mRNA cleavage activity. Our structure of the Piwi–RNA complex, and that determined elsewhere[7], provide direct support for the 5′ region of the guide RNA serving as a nucleation site for pairing with target mRNA and for a fixed distance separating the RISC-mediated mRNA cleavage site from the anchored 5′ end of the guide RNA.

Small interfering RNAs (siRNAs), the cleavage products of RNase III enzyme Dicer, consist of RNA duplexes that contain two-nucleotide 3′ overhangs and 5′-phosphorylated ends. These unique features at the termini of 19–23-base-pair duplexes, which distinguish siRNAs from other endogenous RNAs, are also required for their functional role in RNAi-mediated processes. Extensive structural and biochemical studies on PAZ (for PIWI/Argonaute/Zwille)–RNA recognition[8–10], culminating in the structures of PAZ bound to single-stranded RNA[11] and siRNA-like duplexes[12], have established that the 3′ overhang is specifically recognized by the PAZ domain, a module conserved in both Dicer and Argonaute proteins. Biochemical studies in *Drosophila melanogaster* lysates have shown that the 5′ phosphate on the guide RNA is essential for its assembly into RISC[13,14], whereas related studies have established that the 5′ phosphate of the partner strand is sensed in the process of RISC assembly by means of R2D2 (ref. 15). In addition, the cleavage-site position in the mRNA, paired to the guide RNA in the RISC complex, is defined by the 5′ end of the guide RNA strand[16]. Recent crystal structures have established that the PIWI domain, a highly conserved module in Argonaute proteins, adopts an RNase H fold[4–6]. The Piwi protein also contains within it a conserved basic pocket that probably constitutes the binding site for the 5′ phosphate of the guide RNA[5].

Here we describe the 2.5-Å crystal structure of the *A. fulgidus* Piwi protein (Fig. 1a) bound to a 5′-phosphate-containing 21-mer RNA, capable of self-complementary duplex formation (Fig. 1b). The crystallographic asymmetric unit contains two Piwi proteins, each bound to a short four-base-pair segment of duplex, positioned adjacent to the 5′ phosphate and its attached unpaired nucleotide (Fig. 1c). The structure of the *A. fulgidus* Piwi protein, which consists of a short N-terminal element and two domains labelled A and B (Fig. 1a), is similar (root-mean-square deviation = 0.65 Å for Cα) in the free state[5] and in the RNA-bound complex. The RNA, whose sequence from the 5′ end is p-A1-G2-A3-C4-A5 (Fig. 1b), forms a short A-form duplex, involving pairing of the G2-A3-C4-A5 segment with its complement towards the 3′ end of the sequence (Fig. 1c, d). The RNA duplex is positioned in a basic channel spanning the A–B inter-domain interface of the protein (Fig. 1e), whereas the 5′ phosphate is inserted into a conserved basic pocket located primarily within domain A and the C terminus of domain B (Figs 1e and 2a). A network of hydrogen bonds involving the side chains of Y123, K127, Q137 and K163 and a bound divalent cation anchor the 5′ phosphate into this pocket (Fig. 2a). The bound divalent cation, most probably Mg^{2+}, is octahedrally coordinated to three protein-based oxygens, two nucleic-acid phosphate oxygens and a water molecule in the complex (Fig. 2b). This divalent cation, which is coordinated to the C-terminal carboxylate in an otherwise basic pocket, was also observed in the structure of the free *A. fulgidus* Piwi protein (identified as Cd^{2+})[5], except that two coordinated chlorides are replaced by two phosphate oxygens on complex formation. These results are consistent with the formation of a preformed 5′-phosphate-binding pocket in Piwi, and by extension

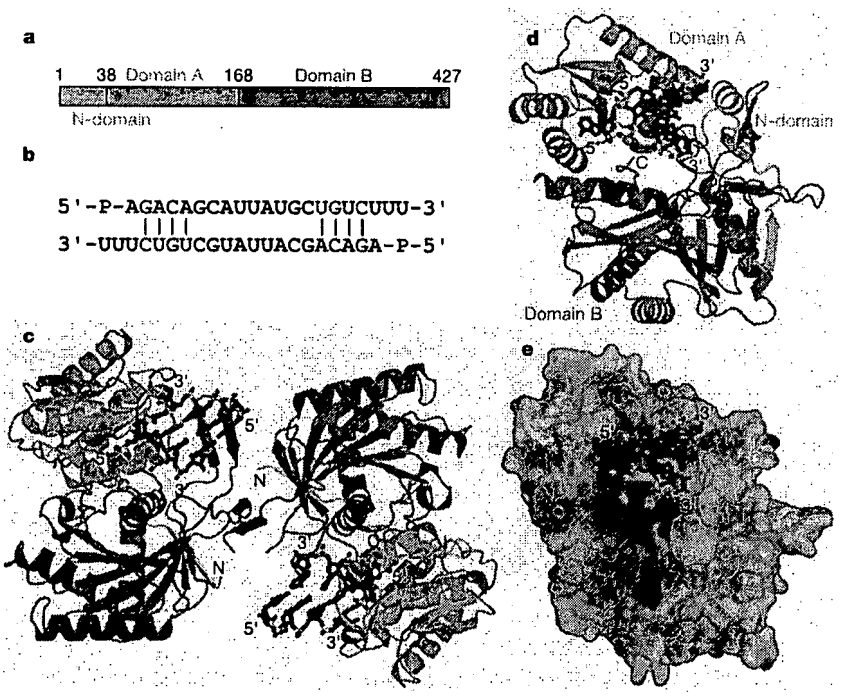

Figure 1 Crystal structure of the *A. fulgidus* Piwi–RNA complex. **a**, The *A. fulgidus* Piwi protein consists of a yellow N-domain (1–37), a magenta domain A (38–167) and a cyan domain B (168–427). **b**, The sequence and pairing alignment of the 21-mer RNA. The red and green segments are observed in the crystal structure of the complex, whereas those in black are disordered. **c**, The relative alignments of the two Piwi proteins together with their bound RNAs within the asymmetric unit. **d**, **e**, Ribbon (**d**) and electrostatic (**e**) views of the complex. The RNA is shown in a stick representation.

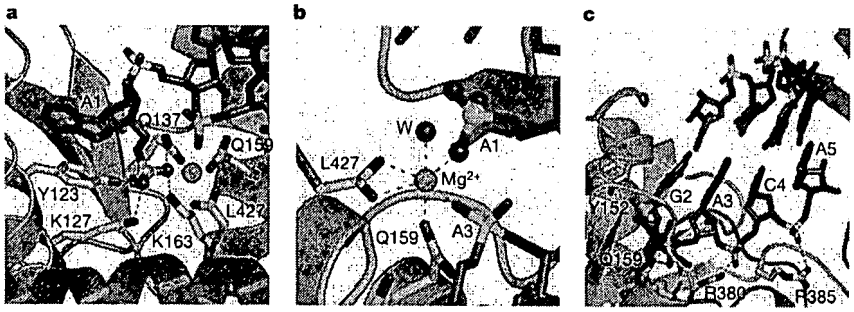

Figure 2 The 5′-phosphate-binding site in the *A. fulgidus* Piwi–RNA complex. **a**, Positioning of the 5′ phosphate in a basic pocket lined by residues of domain A (K127, Y123, Q137, Q159 and K163), domain B (C-terminal L427) and a bound divalent cation in orange. Bases A1 and G2 are splayed apart, with unpaired A1 stacked on Y123. **b**, The octahedral coordination of the bound divalent cation, presumably Mg^{2+}, involving protein and RNA oxygens and a water molecule. **c**, Positioning of the short four-base-pair duplex segment involving the G2-A3-C4-A5 segment (red) with its complementary partner (green). Note intermolecular hydrogen bonds to the non-bridging phosphate oxygens of the A1-G2-A3-C4-A5 segment.

in Argonaute proteins. They also support an earlier prediction of the potential location of the 5′-phosphate-binding pocket within the Piwi scaffold[5].

We propose that it is the guide RNA strand whose 5′ phosphate is anchored in the basic pocket of the Piwi protein. The A1 base at the 5′ end of the guide RNA strand is unpaired and stacks on the aromatic ring of invariant Y123 (Fig. 2a), thereby accounting for non-sequence-specific recognition of the first nucleotide within the 5′-end-binding pocket. The non-bridging oxygens of the backbone phosphates at the A1–G2, G2–A3, A3–C4 and C4–A5 steps are hydrogen-bonded to the side chains of Y152, Q159, R380 and R385, respectively (Fig. 2c). The two paired RNA strands bind in a strongly asymmetric manner, such that the 5′ end of the guide RNA strand (coloured red in Fig. 2c) interacts extensively with the protein, burying 1,500 Å^2 of protein surface, whereas the mRNA strand (coloured green in Fig. 2c) positioned opposite it has minimal contacts with the protein, burying 350 Å^2 of protein surface.

We have generated a set of single and double mutants of *A. fulgidus* Piwi protein residues that contact the 5′ phosphate and attached A1 residue of the bound RNA, in an effort to investigate the importance of these highly conserved residues to RNA recognition. Filter binding studies (averages of three runs)

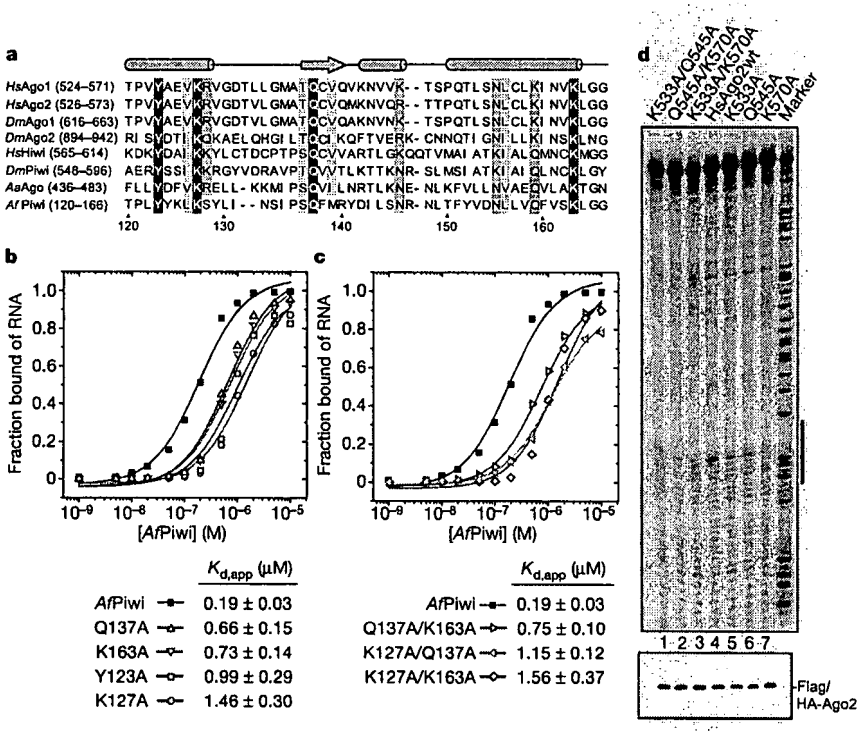

Figure 3 Mutation studies of conserved 5′-phosphate-binding residues in *A. fulgidus* Piwi protein and human Ago2 protein. **a**, Sequence alignment of conserved 5′-phosphate-binding residues across various species of Piwi and Argonaute proteins. Prefix *Hs*, human; *Dm*, *Drosophila*; *Aa*, *Aquifex aeolicus*; *Af*, *Archaeoglobus fulgidus*. **b**, Representative binding curves (average of three runs) for *A. fulgidus* Piwi single-site mutants with 21-nucleotide RNA labelled with 5′-^{32}P by double-filter binding assay. The deduced $K_{d,app}$ values are listed below. **c**, The corresponding binding curves for *A. fulgidus* PIWI dual-site mutants. **d**, The cleavage activities of wild-type human Ago2 and its mutants. The black bar at the right of the image represents the region of the target RNA complementary to the siRNA used. The expression levels of the proteins used in the assays were assessed by western blotting with anti-HA antibody and are shown in the lower panel.

establish that the apparent binding affinity for RNA ($K_{d,app}$) decreases from threefold to sevenfold on proceeding from the wild-type protein (0.19 μM) to mutants Q137A (0.66 μM), K163A (0.73 μM) and K127A (1.46 μM), all of which should disrupt hydrogen bonding to the 5′ phosphate, and mutant Y123A (0.99 μM), which should disrupt stacking with the A1 residue (Fig. 3b). The same trend in binding affinity loss is observed for double mutants Q137A/K163A (0.75 μM), K127A/Q137A (1.15 μM) and K127A/K163A (1.56 μM) (Fig. 3c). These results indicate that 5′ phosphate stabilization might involve multiple hydrogen-bonding interactions and that the disruption of any single interaction or pair of such interactions results in only a modest decrease in binding affinity.

Because the *A. fulgidus* Piwi protein shares significant sequence homology with human Argonaute proteins (Fig. 3a), we mapped the 5′-end-binding pocket in human Ago2, the RISC component that mediates small RNA-guided cleavage of target mRNA[6,17], and set out to investigate whether mutation of key residues lining the 5′-end-binding pocket would affect human Ago2 mRNA cleavage activity. Guided by the crystal structure of the *A. fulgidus* Piwi protein–RNA complex, we introduced single as well as double alanine mutations at the corresponding residues located in the putative 5′-end-binding pocket of human Ago2, namely K533, Q545 and K570 (Fig. 3a). The wild-type human Ago2 guided the cleavage of the radiolabelled target RNA efficiently (Fig. 3d, lane 4). The single alanine mutants, K533A, Q545A and K570A, showed reduced cleavage activity (Fig. 3d, lanes 5 to 7), whereas the double alanine mutants manifested more severe defects in cleavage capacity (Fig. 3d, lanes 1 to 3). These results indicate that the 5′-end-binding pocket observed in *A. fulgidus* Piwi protein is conserved in human Ago2 and is important for its small RNA guided cleavage activity.

We have also directly investigated the effect of 5′-phosphorylation of RNAs on binding affinity. These results, based on a double filter-binding competition assay, establish that the 5′-phosphate-containing RNA (Supplementary Fig. S2a, panels labelled B) binds the *A. fulgidus* Piwi protein about an order of magnitude more tightly than its non-phosphorylated counterpart (Fig. S2a, panels labelled A). It therefore seems that 5′-phosphorylation indeed provides additional affinity for guide RNA recognition of *A. fulgidus* Piwi protein.

There are no specific intermolecular contacts directed to the 2′-OH groups of the RNA in the crystal structure of the *A. fulgidus* Piwi protein–RNA complex, indicating that the Piwi protein might also be targeted by other types of nucleic acid. We have investigated the apparent binding affinities of *A. fulgidus* Piwi protein to both single-stranded and double-stranded 21-mer DNA and RNA oligonucleotides with the use of double filter-binding assays (Supplementary Fig. S2b). The binding is 20-fold tighter for single-stranded DNA than for ssRNA, with the binding affinity decreasing on proceeding from DNA–DNA to RNA–DNA to RNA–RNA duplexes. The preference for ssDNA and dsDNA of the archaeal Piwi protein was unexpected and will need further investigation. Nevertheless, our results are consistent with previous observations that the 2′-OH is not required for RNAi-mediated events[18]. It is also conceivable that other domains within Argonaute proteins and/or other RISC components could provide additional interactions that discriminate between nucleic acid types.

Our structure revealed that the stacked bases 2 to 5 at the 5′ end of the guide RNA are accessible for pairing with their complementary counterparts on the mRNA. Bioinformatics and biochemical analysis of microRNA (miRNA) genes have shown a high degree of sequence conservation restricted to positions 2–8, indicative of a significant contribution of the 5′ end to specificity and activity[19–21]. Our structure supports this concept, in which the mRNA would initially nucleate with the 5′ end of the protein-bound guide RNA strand[19,22], followed by zippering up of the remaining segment to form the guide RNA–mRNA duplex. The observation that the first base on the guide RNA strand is not available for pairing with mRNA in the crystal structure of the complex is consistent with earlier biochemical and kinetic data showing that disruption of this pair has no effect on cleavage activity and under some conditions even favours target cleavage[22].

More than half of the bound 21-mer is disordered in the crystal structure of the *A. fulgidus* Piwi protein–RNA complex (Fig. 1c). We have therefore constructed a model in which the trajectory of the four-base-pair duplex observed in the crystal structure of the complex was extended to form two turns of A-form helix (Fig. 4a). This duplex ends up being positioned within a basic channel[5] that spans one face of both domains A and B of a monomeric Piwi protein (Fig. 4b). The proposed mRNA cleavage site is positioned opposite the putative catalytic residues associated with the RNase H fold of domain B of the Piwi protein[4–6] (Fig. 4a), although the archaeal *A. fulgidus* Piwi protein lacks the DD components of the conserved DDE motif, normally associated with RNase H cleavage activity[23] (Supplementary Fig. S1).

Previous studies have established that the RISC complex cleaves the mRNA strand in a site-specific manner between positions 10 and 11 as defined from the 5′ end of the guide strand[16]. This implies that the catalytic cleavage site is measured from the bound 5′ end of the guide strand by a fixed distance, a feature consistent with the anchoring of both the 5′ phosphate and its adjacent nucleotide of the guide strand, as observed in our structure of the *A. fulgidus*

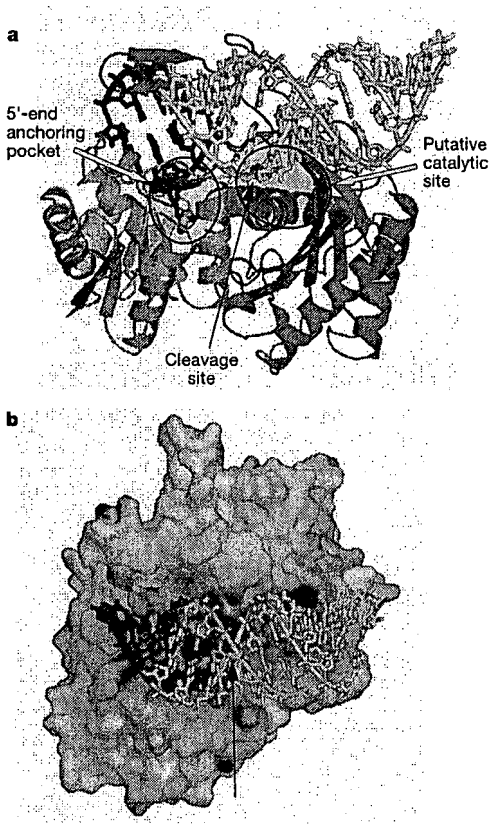

Figure 4 Model of *A. fulgidus* Piwi protein (*Af*Piwi) bound to an 18-base-pair RNA duplex with 5′-phosphorylated single-nucleotide overhangs. **a**, The 5′-end nucleotide and four-base-pair duplex (coloured in red and green for guide strand and target strand, respectively) observed in the crystal structure of the complex were extended by 14-base-pair A-form duplex (coloured in tan and white for guide strand and target strand, respectively). The 5′ end anchoring pocket and putative catalytic site are circled, and the phosphate cleavage site is marked by a red ball. **b**, Electrostatic surface view of the model of the *Af*Piwi–dsRNA complex.

Piwi protein–RNA complex (Figs 2a and 4a).

Argonautes, which contain conserved PAZ and PIWI domains, seem to be the sole proteins required for RISC-mediated activities[24]. Active RISCs, which contain only a single guide RNA strand[25], are capable of directing multiple rounds of site-specific target mRNA cleavage[26]. Both our structure of the *A. fulgidus* Piwi protein–RNA complex and that determined by others[7] provides the first structural insights into 5′ end recognition of the guide RNA strand, the nucleation step associated with guide-RNA–mRNA recognition and the distance-based identification of the mRNA cleavage site. Further attempts at structural characterization of full-length Argonaute–RNA complexes, if successful, could provide structure-based information related to the catalytic cleavage mechanism, a central event of RNA interference. □

Methods

Protein and RNA preparations

The full-length *A. fulgidus* Piwi cDNA was amplified by polymerase chain reaction (PCR) from *Archeoglobus fulgidus* genomic DNA (ATCC) and cloned into pET28a (Novagen) with an amino-terminal His_6 tag. The protein was overexpressed in the *Escherichia coli* host cell BL21-Gold(DE3) (Stratagene) induced by 1 mM isopropyl β-D-thiogalactoside at 20 °C, and purified by Ni-chelating and heparin Hitrap columns. After gel-filtration chromatography on Superdex 200 (Amersham Biosciences), the pure *A. fulgidus* Piwi with attached His tag was concentrated and stored at 30 mg ml^{-1} in 10 mM Tris-HCl pH 8.0, 1 M NaCl and 1 mM dithiothreitol. Selenomethionine-labelled protein was produced by inhibiting the methionine biosynthesis pathway in the host cell. Site-directed mutations were made by a two-step PCR-based overlap extension method and confirmed by DNA sequencing. All the mutants were purified as described for the wild-type protein except that the Heparin column step was omitted. RNAs were synthesized chemically in our laboratory or purchased from Dharmacon, then deprotected and purified by denaturing polyacryamide-gel electrophoresis.

Crystallization and data collection

Crystals of native and selenomethionine-substituted *A. fulgidus* Piwi protein–21-mer RNA complex were grown by hanging-drop vapour diffusion at 20 °C. About 15 mg ml^{-1} protein–RNA complex in 0.1 M KCl, 10 mM HEPES-K pH 7.5 buffer was mixed 1:1 with a well solution containing 6% polyethylene glycol 4000, 40 mM KCl, 10 mM $MgCl_2$ in 50 mM sodium cacodylate pH 6.5. These crystals grew to a maximum size of 0.2 mm × 0.2 mm × 0.2 mm over the course of 10 days.

For data collection, crystals were flash frozen (100 K) in the above reservoir solution supplemented with 30% glycerol with a 10% step increase. A total of 720 frames of 0.5° oscillation were collected on the 2.5 Å crystals of selenomethionine-labelled *A. fulgidus* Piwi protein–21-mer RNA complex at 0.9776 Å at National Synchrotron Light Source (NSLS) beamline X26C, Brookhaven National Laboratory. The data were processed with HKL2000 (http://www.hkl-xray.com/). The crystal belonged to space group *R*3, with unit cell parameters listed in Supplementary Table S1. There were two complex molecules per asymmetric unit, with about 55% solvent content.

Structure determination

The structure of the *A. fulgidus* Piwi protein–21-mer RNA complex was solved by using the free *A. fulgidus* Piwi protein structure (PDBID: 1W9H) as the search model and Molrep (CCP4 package)[27] was used to locate the two copies of the *A. fulgidus* Piwi protein. The extra density corresponding to the 5′ terminus of the RNA and several additional base pairs could be clearly traced without ambiguities from the earliest stage. The *A. fulgidus* Piwi protein–RNA complex model was rebuilt with the program O[28] and refined with CNS (http://cns.csb.yale.edu/v1.1/) and REFMAC (CCP4 package)[27]. The R-free set contained 5% of the reflections chosen at random. Refinement statistics are given in Supplementary Table S1. The protein comprises residues 2–427 and the RNA comprises the 5′ phosphate, the A1 residue and four additional base pairs involving residues at the 5′ end. Disordered regions within the *A. fulgidus* Piwi protein included loop segments 304–308 and 331–341 for molecule A and 332–338 for molecule B in the asymmetric unit. The middle part of the duplex RNA (nine base pairs) and three nucleotides at the 3′ end cannot be traced in our final density map. The figures were prepared with PyMOL (http://pymol.sourceforge.net/).

Double filter-binding assays

The affinity of the *A. fulgidus* Piwi and its mutants for various oligonucleotides was detected and quantified with a double filter-binding assay[29]. The reactions containing 5′-^{32}P-labelled nucleic acids and proteins were applied to filters containing two membranes: a protein-binding Protran BA-85 nitrocellulose membrane and a nucleic-acid-binding Hybond-N^+ nylon membrane. After air-drying, the filters were quantified on a PhosphorImager. The data were analysed as reported previously[30]; details of experimental protocols are listed in Supplementary Methods.

Cleavage assays using human Ago2 and its mutants

The Flag/haemagglutinin (HA)-tagged wild-type and mutant constructs were transiently transfected into HEK-293 cells, and Ago2 proteins were immunoprecipitated from the cell lysates with anti-Flag antibody. The expression levels of the wild-type and mutant Ago2 proteins were assessed by western blotting with anti-HA antibody (Fig. 3c, lower panel). The stringently washed beads carrying equal amounts of bound Flag/HA-tagged human Ago2 proteins were preincubated with a single-stranded siRNA to reconstitute RISC activity. After an additional washing step to remove the unbound siRNA, the beads were incubated with a ^{32}P-cap-labelled target RNA. After incubation for 1 h the RNA was recovered from the beads and analysed by denaturing gel electrophoresis. Details of the experimental protocols are listed in Supplementary Methods.

Received 6 February; accepted 10 March 2005; doi:10.1038/nature03514.

1. Hutvagner, G. & Zamore, P. D. RNAi: nature abhors a double-strand. *Curr. Opin. Genet. Dev.* **12**, 225–232 (2002).
2. Hannon, G. J. RNA interference. *Nature* **418**, 244–251 (2002).
3. Meister, G. & Tuschl, T. Mechanism of gene silencing by double-stranded RNA. *Nature* **431**, 343–349 (2004).
4. Song, J. J., Smith, S. K., Hannon, G. J. & Joshua-Tor, L. Crystal structure of Argonaute and its implications for RISC slicer activity. *Science* **305**, 1434–1437 (2004).
5. Parker, J. S., Roe, S. M. & Barford, D. Crystal structure of a PIWI protein suggests mechanisms for siRNA recognition and slicer activity. *EMBO J.* **23**, 4727–4737 (2004).
6. Liu, J. *et al.* Argonaute2 is the catalytic engine of mammalian RNAi. *Science* **305**, 1437–1441 (2004).
7. Parker, J. S., Roe, S. M. & Barford, D. Structural insights into mRNA recognition from a PIWI-domain–siRNA guide complex. *Nature* doi:10.1038/nature03462 (this issue).
8. Yan, K. S. *et al.* Structure and conserved RNA binding of the PAZ domain. *Nature* **426**, 468–474 (2003).
9. Lingel, A., Simon, B., Izaurralde, E. & Sattler, M. Structure and nucleic-acid binding of the *Drosophila* Argonaute 2 PAZ domain. *Nature* **426**, 465–469 (2003).
10. Song, J. J. *et al.* The crystal structure of the Argonaute2 PAZ domain reveals an RNA binding motif in RNAi effector complexes. *Nature Struct. Biol.* **10**, 1026–1032 (2003).
11. Lingel, A., Simon, B., Izaurralde, E. & Sattler, M. Nucleic acid 3′-end recognition by the Argonaute2 PAZ domain. *Nature Struct. Mol. Biol* **11**, 576–577 (2004).
12. Ma, J. B., Ye, K. & Patel, D. J. Structural basis for overhang-specific small interfering RNA recognition by the PAZ domain. *Nature* **429**, 318–322 (2004).
13. Nykänen, A., Haley, B. & Zamore, P. D. ATP requirements and small interfering RNA structure in the RNA interference pathway. *Cell* **107**, 309–321 (2001).
14. Tomari, Y. *et al.* RISC assembly defects in the *Drosophila* RNAi mutant Armitage. *Cell* **116**, 831–841 (2004).
15. Tomari, Y., Matranga, C., Haley, B., Martinez, N. & Zamore, P. D. A protein sensor for siRNA asymmetry. *Science* **306**, 1377–1380 (2004).
16. Elbashir, S. M., Lendeckel, W. & Tuschl, T. RNA interference is mediated by 21- and 22-nucleotide RNAs. *Genes Dev.* **15**, 188–200 (2001).
17. Meister, G. *et al.* Human Argonaute2 mediates RNA cleavage targeted by miRNA and siRNAs. *Mol. Cell* **15**, 185–197 (2004).
18. Chiu, Y. L. & Rana, T. M. siRNA function in RNAi: a chemical modification analysis. *RNA* **9**, 1034–1048 (2003).
19. Mallory, A. C. *et al.* MicroRNA control of PHABULOSA in leaf development: importance of pairing to the microRNA 5′ region. *EMBO J.* **23**, 3356–3364 (2004).
20. Lewis, B. P., Burge, C. B. & Bartel, D. P. Conserved seed pairing, often flanked by adenosines, indicates that thousands of human genes are microRNA targets. *Cell* **120**, 15–20 (2005).
21. Doench, J. G. & Sharp, P. A. Specificity of microRNA target selection in translational repression. *Genes Dev.* **18**, 504–511 (2004).
22. Haley, B. & Zamore, P. D. Kinetic analysis of the RNAi enzyme complex. *Nature Struct. Mol. Biol.* **11**, 599–606 (2004).
23. Yang, W. & Steitz, T. A. Recombining the structures of HIV integrase, RuvC and RNase H. *Structure* **3**, 131–134 (1995).
24. Rand, T. A., Ginalski, K., Grishin, N. V. & Wang, X. Biochemical identification of Argonaute2 as the sole protein required for RNA-induced silencing complex activity. *Proc. Natl Acad. Sci. USA* **101**, 14385–14389 (2004).
25. Martinez, J., Patkaniowska, A., Urlaub, H., Luhrmann, R. & Tuschl, T. Single-stranded antisense siRNAs guide target RNA cleavage in RNAi. *Cell* **110**, 563–574 (2002).
26. Hutvagner, G. & Zamore, P. D. A microRNA in a multiple-turnover RNAi enzyme complex. *Science* **297**, 2056–2060 (2002).
27. Collaborative Computational Project no. 4. The CCP4 suite: programs for protein crystallography. *Acta Crystallogr. D* **50**, 760–763 (1994).
28. Jones, T. A., Zou, J. Y., Cowan, S. W. & Kjeldgaard, G. J. Improved methods for building protein models in electron density maps and the location of errors in these models. *Acta Crystallogr. A* **47**, 110–119 (1991).
29. Wong, I. & Lohman, T. M. A double-filter method for nitrocellulose-filter binding: Application to protein-nucleic acid interactions. *Proc. Natl Acad. Sci. USA* **90**, 5428–5432 (1993).
30. Sagar, M. B., Lucast, L. & Doudna, J. A. Conserved but nonessential interaction of SRP RNA with translation factor EF-G. *RNA* **10**, 772–778 (2004).

Supplementary Information accompanies the paper on **www.nature.com/nature.**

Acknowledgements We thank A. Saxena and personnel at synchrotron beamline X26C of the National Synchrotron Light Source (NSLS), Brookhaven National Laboratory, for their assistance. Use of the NSLS beamline is supported by the US Department of Energy, Basic Energy Sciences, Office of Science. D.J.P. is supported by funds from the Abby Rockefeller Mauze Trust and the Dewitt Wallace and Maloris Foundations, and T.T. is supported by a National Institutes of Health grant.

Competing interests statement The authors declare that they have no competing financial interests.

Correspondence and requests for materials should be addressed to D.J.P. (pateld@mskcc.org). Coordinates have been deposited in the Protein Data Bank under accession code 1YTU.